Available online at www.easdprocedia.org
EASD Procedia EURODYN (2020) 3053-3066

EASD Procedia

EURODYN 2020
XI International Conference on Structural Dynamics
M. Papadrakakis, M. Fragiadakis, C. Papadimitriou (eds.)
Athens, Greece, 23–26 November 2020

A GROUND MOTION MODEL FOR SEISMIC VULNERABILITY ASSESSMENT OF PROTOTYPE INDUSTRIAL PLANTS

C.Nardin[1], R.di Filippo[1], R.Endrizzi[1], I. Lanese[2], F.Paolacci[3], O.S.Bursi[1]

[1]University of Trento, Department of Civil, Environmental and Mechanical Engineering
via Mesiano 77, 38123 Trento, Italy
e-mail: chiara.nardin@unitn.it

[2] EUCENTRE Foundation
Via Adolfo Ferrata 1, 27100 Pavia, Italy

[3] Roma Tre University Department of Engineering
Via Vito Volterra 62, 00146 Rome, Italy

Keywords: Ground motion model, industrial plants, shaking table tests.

Abstract. *Relationships between seismic action, system response and relevant damage levels in industrial plants require a solid background both in experimental data, due to the high level of nonlinearity, and in knowledge of seismic input due to large uncertainty. Besides, risk and fragility analyses depend on the adoption of a huge number of seismic records usually not available in a site-specific analysis. In order to manage these issues and to gain knowledge on the definition of damage levels, limit states and performance for major-hazard industrial plant components, we present a possible approach and discuss results of an experimental campaign based on a real prototype industrial steel structure. The investigation of the seismic behaviour of the reference structure has been carried on through shaking table tests, focusing in particular on the structural or process-related interactions that can lead to serious secondary damages as leakage in piping systems or connections with tanks and cabinets. This has been possible thanks to the adoption of a ground motion model (GMM) able to generate a suite of synthetic time-histories records for specified site characteristic and earthquake scenarios. In fact, model parameters can be identified by matching the statistics of a target-recorded accelerogram to the ones of the model in terms of faulting mechanism, earthquake magnitude, source-to-site distance and site shear-wave velocity. Hence, the stochastic model, based both on these matched parameters and on filtered white-noise process, generates the ensemble of synthetic ground motions capable to capture the main features of real earthquake ground motions, including intensity, duration, spectral content and peak values. Finally, by means of the combination of a high-fidelity and a low-fidelity FE model as well as the stochastic input generated by a GMM, a seismic vulnerability assessment of both industrial components and the global structure can be carried out.*

ISSN:2311-9020 © 2020 The Authors. Published by EASD Procedia.
Peer-review under responsibility of the Organizing Committee of EURODYN 2020.
doi: 10.47964/1120.9249.19159

INTRODUCTION

Between major natural hazard critical for industrial facilities, we can undeniably enlist seismic events. In fact, as well documented in literature - see [1]; [2]; [3] -, in these occurrence, industrial process plants have shown to be susceptible to experience significant damages both in primary structure and in secondary elements that usually constitute plant components and on which rely the operation of facilities.

Besides, as demonstrated by recent catastrophic events - like Tohoku earthquake in 2011 - and particularly stressed in the literature - see [4]; [5] - industrial facilities are especially vulnerable to those natural hazards which may trigger technological accidents: the so called NaTech events, i.e. Natural-Technological events. Therefore, there is a strong necessity to investigate interactions between primary structure and plant components, but also between the components among themselves, in order to avoid, as shown in previous references, serious consequences and critical secondary damages which, in addition to loss of production, also pose a danger to humans and the environment if hazardous substances are released due to leakages. In this perspective, the objective of the project SPIF, i.e. *Seismic Performance of Multi-Component Systems in Special Risk Industrial Facilities*, under the grant of European H2020 - SERA, *Seismology and Earthquake Engineering Research Infrastructure Alliance for Europe*, is to carry out a complete investigation of the seismic behaviour of industrial plants equipped with complex process technology by means of shaking table tests.

The case-test structure is a three-storey moment resisting steel frame with vertical and horizontal vessels and cabinets, arranged on the three levels and connected by pipes. The three levels are constructed as flexible diaphragm made of steel cross beams, partially covered with gratings. Tests are carried out without base isolation of the industrial structure. Furthermore, firmly anchored components are taken into account to compare their dynamic behavior and interactions with each other. Besides, the campaign structure is equipped with sensor systems integrated into the test structure itself for a rapid damage assessment.

Along with this line, the following paper focuses on the main aspects of investigation of seismic performances of a prototype steel-frame industrial plant, with a special focus on loss of containment (LoC) from bolted flange joints (BFJs), see [6], pipe bends and tee-joints, vessels' connections and anchorages. Therefore, seismic risk is evaluated through fragility curves analyses, according to [10] inside the framework of PBEE, [8].

In details, to take into account the variability of the seismic action and the high number of time histories needed, a GMM has been adopted, in order to generate a suite of synthetic time-histories records for specified site characteristic and earthquake scenarios, based on the results of a site-specific probabilistic seismic hazard analysis in severe seismic prone zone in Italy - PSHA, see [7].

Moreover, a faster-low (LF) and a refined high fidelity (HF) FE models are developed in order to represent the complexity of the experimental campaign with two different level of computational efforts and accuracy reproduced. The whole test campaigns provide then the necessary background to properly calibrate FE models. Therefore, in order to reduce the space of the GMM parameters, a global sensitivity analysis (GSA) over FE models is performed to assess the individual contributions of each input variables to the total variance of the model response. Finally, the LF model of the prototype industrial plant is adopted to perform a seismic fragility analysis with a cheaper computational effort demanded.

In sum, the paper is arranged into 6 main sections: the first section illustrates SPIF test structure, whilst the second one focuses on the characterization of the seismic input. The third

section presents the arrangement of the experimental campaign, in the fixed configuration. The fourth one deals with the description of the FE modelling of the primary structure and of the industrial components, such as pipes, bends and vessels. In the fifth section, we show the procedure in order to gain relevant seismic fragility curves both for components and the global system. In the last section, main conclusions are drawn and future developments are proposed.

THE SPIF STRUCTURE

The primary steel structure is a three storey moment resisting steel frame with flexible diaphragm made of crossbeams. The three dimensional primary steel structure is shown in Fig. (1). The ground-plan dimensions are 3.7 m x 3.7 m and the storey height is 3.1 m, which leads to a total height of 9.3 m. The rigid frame is simply supported on the reinforced concrete base plate and the crossbeams are hinged connected to the frame beams. In total four tanks are installed, two vertical tanks on the first level and two horizontal tanks on the second level. Furthermore one electrical cabinet is placed on the first level. Concerning piping system, the nominal pipe diameter is DN 100, with the exception of the suspended pipes on the third story that are DN 80. In addition, smaller single degree of freedom (SDOF) oscillators systems are installed on each of the three levels to investigate the structure component interaction for different periods in the linear and non-linear range.

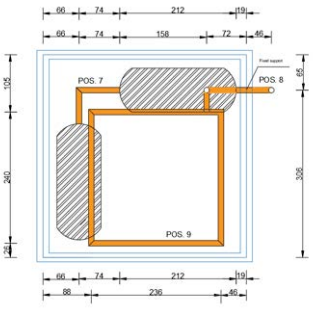

(a) Top view.

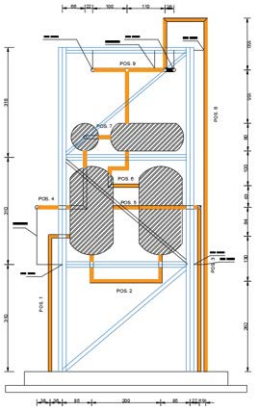

(b) Side view.

(c) 3D front view.

(d) 3D back view.

Figure 1: Representation with quote of the prototype industrial plant for SPIF project: (a) top, (b) side and (c)-(d) 3D front and back views.

Besides, the test structure is equipped with a complex system of sensors which includes FBG

fiber optics sensors, for LoC and leakage detection, strain-gauges, LVDT and accelerometer in strategical positions, as shown for example in Fig. (2).

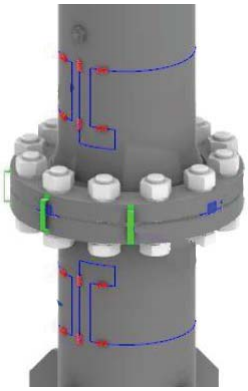

(a) FBG sensors.

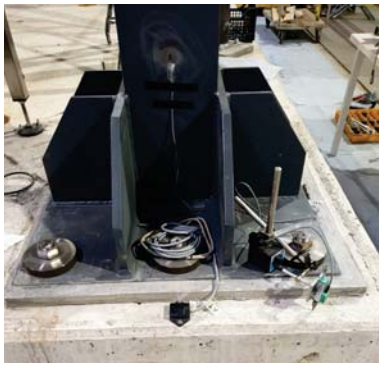

(b) Accelerometers at base joint.

Figure 2: Part of system's sensors applied to test structure: in more detail, (a) FBG sensors connected to flange susceptible to leakage phenomena, (b) disposition of accelerometer at base joint of the primary steel structure.

EXPERIMENTAL CAMPAIGN

Sequence and intensity levels of shaking table tests are performed so as to reach more severe damages or even collapses in components by passing from *fully operational* (OP) to *near collapse* (NC) limit states, or, as in case of major industrial plants, from *operating condition or design basis earthquake condition* (OBE) to *safe shutdown earthquake condition* (SSE). In particular, the first set of simulation tests are executed on the base isolated structure while the second set is run on the non-isolated configuration. In both configuration's setup, after tuning the shaking table, input signals are launched and then scaled with coefficient related to the probability of exceeding the seismic action, P_L, in T_L years other than the reference probability of exceedance P_{LR}, over the same T_L years, as reported in Tab. (2). In more details, according to

	Components EC8-4:(2.1.4)	**Buildings** EC8-4:(4.2.5)
Cl. I	0.8	0.8
Cl. II	1	1
Cl. III	1.2	1.2
Cl. IV	1.6	1.4

Table 1: Important class and coefficients according to EC8, Part 1 and Part 4.

the assumption during design phase of considering an importance factor γ_I equal to 1.0, it has been evaluated in Eq. (1) the ratio between the maximum allowed value of importance factor in case of components versus the assumed one, see Tab. (1): this ratio is then used as a scale factor in order to pass to a SLS *safe life limit state* for the structure and the equivalent OBE *operating condition or design basis earthquake condition* for pipe systems.

$$\gamma_I = \frac{1}{1.6} = 0.625 \tag{1}$$

Probability of Exceedance NTC18: 3.2.1			
OP	81	%	Fully Operational
DL	63	%	Damage Limit
SD	10	%	Significant Damage
NC	2.5	%	Near Collapse

Table 2: Probability of exceedance according to Italian Standards.

Then, according to EC8-Part 1: (2.1-4(P)Note), the value of the importance factor γ_I is obtained by the ratio between T_L and T_{LR}, i.e. time associated to the reference seismic action in order to achieve the same probability of exceedance in T_L years as in the T_{LR} years for which the reference seismic action is defined

$$\gamma_l = \left(\frac{T_{LR}}{T_L}\right)^{-1/k} with \quad k = 3 \tag{2}$$

as well as

$$\gamma_l = \left(\frac{P_L}{P_{LR}}\right)^{-1/k} with \quad k = 3 \tag{3}$$

again the needed factor with which multiply the reference seismic action. So, by referring to Italian codes in Tab. (2), importance factors for different limit states are evaluated and reported in Tab. (3), together with the reference peak ground acceleration of the spectra involved in the design phase. Main assumptions in order to evaluate proper spectra for the test structure were

	NC	**SD**	**DL**	**OP**	**units**
γ_I	1.000	0.625	0.541	0.498	[-]
a_{gR}	0.690	0.431	0.233	0.215	[g]
	SSE	**OBE**			

Table 3: Important coefficients and reference peak ground acceleration for different limit states.

in fact the following ones: · nominal life: 50 years; · soil type: C –T1; · damping: 5%; · peak ground acceleration: $a_{gR} = 0.69\,g$ and · importance class II.

Therefore, spectra-compatible accelerograms have been evaluated with a relative difference between matched and target spectra less than 10%. These accelerograms are assigned to both the configuration setup, i.e. structure with and without base isolation, with the 4 aforementioned different scale factors related to separated limit states.

Furthermore, for the isolated setup, natural records from PEER NGA-WEST2 database are selected, with the purpose of stressing the designed isolators. In particular, selection criteria were devoted to have a strong frequency content around the range of the working-isolated structure and to match the design spectrum. For this last point, it has been necessary to scale up the natural accelerogram selected with the first main issue, according to a scale factor derived as the ratio between maximum acceleration reached by the artificial seismic input and the natural one.

Then, in order to induce damage or collapse in previous analysed components, as, for example, leakage in selected flanges or collapse of vessel's footing, seismic records from ground

motion model are selected, thanks to the high variability of the ensemble site-characteristic generated. Hereafter, the main characteristics and peculiar aspects of the ground motion model are presented.

SEISMIC INPUT FROM GMM

Synthetic ground motions are employed in order to cover the range of IMs of interest and eventually obtain a sufficient large ensemble of time-histories for fragility curves analyses. Here, a synthetic ground motion model has been assumed in order to reproduce the spectral variability of recorded accelerograms. In particular, according to [9], with the purpose of calibrating the GMM for a specific geographical location and specific site characteristics, a PSHA deaggregation is performed. Along this line, in the assumption of far-field scenario, a severe seismic prone zone of central Italy is selected. Below, see Fig. (3), it is reported the main result of the probabilistic seismic hazard deaggregation analysis.

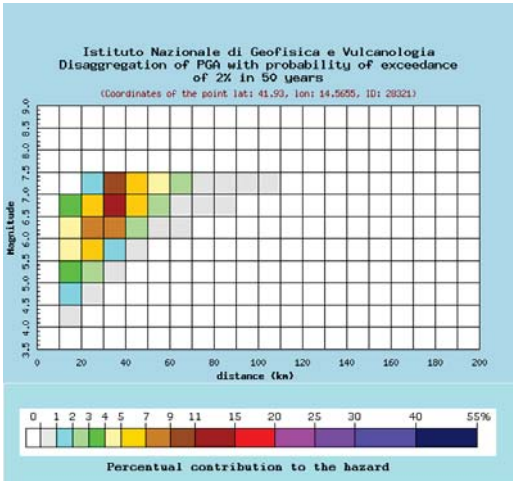

Figure 3: Probabilistic seismic hazard deaggregation analysis for Palmoli, Central Italy.

Moreover, the original recorded accelerograms are selected from the INGV site (http://www.ingv.it/) and ITACA - *Italian Accelerometric Archive* - Database, with the following criteria:

- fault to site distance $> 10\ km$;
- moment magnitude > 5.5;
- main shock seismic records only.

Besides, another core assumption, both in design of the structure and in selection of ground motions time histories, is correlated to the soil characteristics, that is assumed of type C according to European standards. Herein, in Tab. (4) compatible accelerograms are reported.

According to [11], GMM is defined in terms of a set of parameters based on ground motion properties with physical meaning, as reported in Tab. (4). The model is based on a modulated, filtered white-noise process and incorporates both temporal and spectral non-stationarities, as shown in Eq. (4)

$$a_g(t) = q(t,\alpha)\left[\frac{1}{\sigma_f(t)}\int_{-\infty}^{t} h(t-\tau,\lambda(\tau))\,\omega(\tau)d\tau\right] \tag{4}$$

	Earthquake Name	Station Name	$V_{S,30}[m/s]$	Distance fault-site $[km]$	Moment Magnitude $[M_w]$
1	IT-1979-0009-NORCIA	BVG	211	38	5,8
2	IT-1984-0004-LAZIO-ABRUZZO	CSN0	501	19,7	5,9
3	IT-1984-0004-LAZIO-ABRUZZO	PNT	325	26,8	5,9
4	IT-1984-0004-LAZIO-ABRUZZO	GRG2	187	49,1	5,9
5	IT-1984-0004-LAZIO-ABRUZZO	GRG1	192	49,1	5,9
6	IT-2009-0009-L-AQUILA	AVZ	199	35,1	5,5
7	IT-2009-0009-L-AQUILA	GSA	492	14,4	5,5
8	EMSC-20160824-CENTRAL-ITALY	TRE	353	45,3	6
9	EMSC-20160824-CENTRAL-ITALY	FOC	342	45,7	6

Table 4: Set of selected accelerograms from ITACA database.

where $\omega(\tau)$ is a white-noise process, while $\widehat{\alpha}$ is defined by means of

$$\widehat{\alpha} \, = \, arg \min_{\alpha} \left(\left| I_a \left(t_{45} \right) \, - \, \widehat{I}_a \left(t_{45} \right) \right| \, + \left| \left(t_{95} \right) \, - \, \widehat{I}_a \left(t_{95} \right) \right| \right) \tag{5}$$

It should be noticed that the modulating function $q(t, \alpha)$ completely defines the temporal characteristics of the process, whereas $h\left(t \, - \, \tau, \lambda(\tau)\right)$, denoting the impulse-response function IRF, and its time-varying parameters define the spectral characteristics of the process. In particular, IRF of a linear time-varying filter can be expressed as follows:

$$h\left(t \, - \, \tau, \lambda\left(\tau\right)\right) \, = \, f(\omega_f, \zeta_f) \tag{6}$$

where

$$\omega_f \, = \, \omega_{mid} \, + \, \omega'(t \, - \, t_{mid}) \tag{7}$$

Simulating process of GMM is then able to generate an ensemble of ground acceleration time-history similar to those illustrated in Tab. (4) for a given set of model parameters, as reported in Tab. (5).

Name	Distribution	Average Value	Units
I_a	Uniform	0,212	$[m/s]$
t_{mid}	Uniform	3,6	$[s]$
D_{5-95}	Uniform	8,8	$[s]$
ω_{mid}	Uniform	43,7	$[Hz]$
ζ_f	Uniform	0,25	$[-]$

Table 5: Distribution of stochastic GMM parameters.

Along this line, two main hyphotesis have been assumed: the first one is to consider parameters statistically independent; the second regards the choice of assuming uniform distributions in order to describe probability distribution of all the parameters, with the only exception of ω' that is assumed constant. Thus, in order to reduce the variability of the seismic input and to reduce the space of parameters, a set of 200 white-noises combining 200 accelerograms is performed on the LF model with a convergence check upon the third quartile of both spectral acceleration for $T_1 \, = 0.36 \, s$ and maximum displacement at top storey. Results are reported in Fig. (4) and Fig. (5) and indicate that at almost 100 of white-noises convergence is reached.

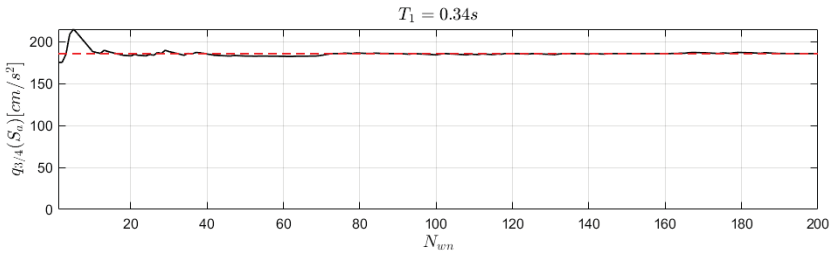

Figure 4: Check on number of white-noises N_{wn} at the third quartile for $S_a(T_1)$.

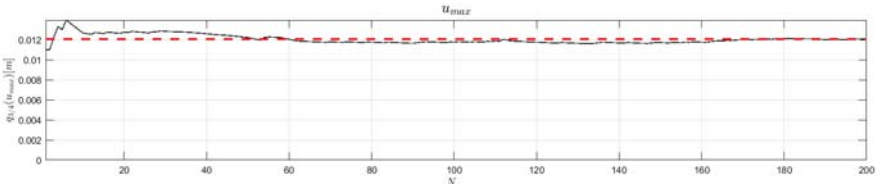

Figure 5: Check on number of white-noises N_{wn} at the third quartile for u_{max} at top storey.

THE FINITE ELEMENT MODEL

According to [9], one of the most important feature of a GMM is the possibility to study the structural response to earthquake with characteristics that are coherent with the site seismicity (e.g. fragility curves). The main disadvantage of this technique is the great number of non linear analysis necessary to take into account the variability of the seismic action. To overcome the numerical effort required in such procedure two model are needed.

First a low fidelity model (LF) that aims to reproduce the essential characteristics of the system with the smallest computational effort possible is developed. For our purposes this essential characteristics are: natural periods, base shear and behaviour of the major component such as tanks and piping system.

In a second phase an high fidelity model (HF) is introduced with the purpose to caught the behaviour of the structure in greater detail even with reference to the interaction between primary and secondary elements.

In the next section, only issues and principal techniques involved in the definition of LF and HF model of the isolators are discussed, while a general comment on the main differences between LF and HF model is briefly dwell.

Piping system

As can be seen in Fig. (1) the piping system is composed of straight pipes, bends, tee joint and BFJs. Since our purpose is to include in the model only the foundamental aspects of the structure, we firstly have to identify the most critical components for the LoC limit state. According to [14] there are only three possible failure modes for pipes: fracture due to excessive tensile loading, local buckling due to compressive action and low cycle fatigue. The first failure mode is prevent if the plastic deformation does not exceed the tensile strain limit ϵ_{Tu}, that the Author suggests to use a conservative value of 2%. Compressive failure is typical in pipe bends and the limit compression strain ϵ_{Cu} can be estimated from Eqn. (8)

$$\epsilon_{Cu} = 0.5 \cdot \left(\frac{t}{D}\right) - 0.0025 + 3000 \cdot \left(\frac{\sigma_h}{E}\right)^2 \tag{8}$$

Neglecting the effect of internal pressure, a value of 1% is found. Instead, the third failure

mode arises only if the component undergoes large plastic deformation several times. Thanks to results of preliminary analysis, it is possible to outline only two points (the nozzle in position 6 and the tee joint in position 5) with tension's value above yielding limit. To investigate the possibility of high stress level, those position are model with *shell finite elements*. It is important to notice LF model is an elastic one, since the structure is designed to remain elastic even under very high seismic shacking. In later analysis the elastic solution will be used as guide to choose significant ground motions to evaluate inelastic response of components. In conclusion, such level of deformation in pipes capable to induce failure seems to be unlikely. So, the weakest component for the LoC prevention are the BFJs. The model proposed by [15] is used to investigate the performance of the BFJs. This method is developed in the framework of the EN 1591-2009 and results in a linear domain like the one shown in Fig. (6). The BFJs are designed in accordance with EN 1591-2014 to ensure the performance level requested in two seismic condition:

- Operating condition basis earthquake **(OBE)**: it corresponds to an earthquake scenario, considering the seismic hazard of the site, that could reasonably affects the structure during his operating life time;
- Safe shut-down earthquake **(SSE)**: it corresponds to maximum ground motion for which some critical components of the plant must be designed to remain functional.

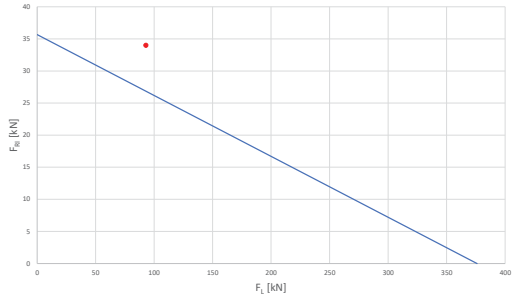

Figure 6: Example of leakage domain of the La Salandra model

To model the rest of the piping system in terms of mass and stiffness, several techniques are available. The easiest choice is to adopt beam element with reduced stiffness' value by means of flexibility factors. Codes provide an analytical formulation of these factors based on elasticity theory. Example of such factors, in the case of elbow element, are shown in equations below.

$$h = \frac{4 \cdot R \cdot e_n}{d_m^2} \tag{9}$$

$$k_B = \frac{1,65}{h} \tag{10}$$

In case of tee joint, no stiffness reduction is required. A more precise approach consist in the determination of flexibility factors for elbows derived from a FEA. In this case a FEM of pipe bends based on shell element is developed and moments are applied to one end. Then, by equating deflection of the FE model with an analogous system of beam deflection, it is possible to evaluate proper flexibility factors. According to [16] using this procedure flexibility factors

Flexibility factor		
Direction	UNI EN 13480-3	FEM
In plane	9.24	8.28
Out of plane	9.24	8.21

Table 6: Comparison between flexibility factor

Figure 7: FEM of a single elbow

for in plane and out of plane action can be found. The results of the two procedure are resumed in Tab. (6), while FE model employed is depicted in Fig. (7).

In this calculation, stiffening effects of pressure are neglected, since just few elbows are pressurized and with a negligible resultant effect caused by internal pressure.

The main hypothesis by referring to flexibility factor is that the ends of the elbow are free to ovalize. Thus, if this condition is not respected, a significant stiffening effect raise. In order to individuate those critical conditions, a parametric study is carried out with this scheme: a specimen made of two elbows (with direction specified in Tab. (7)) separated by a straight pipe is analysed. Several simulations are launched for increasing length of the central pipe from 200mm to 3000mm. During the simulation, two set of displacement are imposed to the specimen: a linear displacement parallel to the straight pipe and a rotation of one end. As a result mutual force to the imposed displacement are collected. For high length of central pipe, flexibility contribution for elbow is constant and the central pipe behaves like a beam with circular cross section. When the length of central pipe goes under a threshold value, a stiffening effect can be seen and also induce an error greater than 10%, compared to the equivalent beam behaviour. Thus, a cut-off length can be defined.

Bends scheme	Direction	L [mm]
L-R	Axial	450
	Bending	200
L-L	Axial	450
	Bending	300
L-U	Axial	450
	Bending	450

Table 7: Cut-off length

Looking at Tab. (7), it is possible to notice that in case of bending a cut-off length equal to $2,5D$ is adequate. This result are in good agreement with results of [16]. In the other cases, when forces are of primary importance, a greater value of $4D$ looks adequate.

FRAGILITY ASSESSMENT OF A STEEL STRUCTURE AND COMPONENTS

In this paragraph, a method for performing fragility assessment of components and structure is illustrated, based on the seismic response of the test structure on the LF model. In fact, by using outputs of the simulations, it is possible to evaluate fragility functions F_D defined as the conditional probability of an event - i.e. overpass a threshold for a certain damage state (D) - given the observation of an intensity measure (IM) which describes the seismic event, see [7] and [10].

$$F_D\left(im\right) \, = \, P\left[D \geq C_{LS} | IM \, = \, im\right] \tag{11}$$

So, it is clear the importance of the choice of both the intensity measure proper for the case-test and the definition of the damage state D and its class of limit state C_{LS}, seen as thresholds - [17].

The most popular procedure to compute fragility functions via time-history analysis can be summarized, according to [18] and [19], as follows:

- definition of a numerical model for the structure of interest, $y(t) \, = \, \mathcal{M}[\ddot{x}_g(t|IM \, = \, im); \theta_{\mathcal{M}(t)}]$ where $\mathcal{M}$ stands for the numerical model, $\theta_{\mathcal{M}}$ for a set of model parameters, and $\ddot{x}_g$ for the seismic input;
- selection of suitable IM and N ground motions of interest;
- selection of EDP of interest;
- definition of damage limit states D via EDP thresholds.

Given the N outcomes, it is common to assume a lognormal probability distribution for the random variable IM associated with the given damage state D. Then, the parameter of the lognormal can be estimated via the method of the maximum likelihood. However, one positive aspect of the likelihood function is that it can be written also for a generic probability density function $f(x;\theta)$, where θ is the set of parameter to be estimated. Thus, by dividing data into two groups, i.e. data that causes collapse and data that do not cause collapse, the likelihood function is given by:

$$\mathcal{L}\left(\theta\right) \, = \, \prod_{n=1}^{N} f\left(x;\theta\right)^{\overline{N}} \left[\, 1 \, - \, F\left(\overline{x};\theta\right)\right]^{\left(N \, - \, \overline{N}\right)} \tag{12}$$

or in logarithmic form

$$ln\mathcal{L}\left(\theta\right) \, = \, \sum_{n=1}^{N} f\left(x;\theta\right) \, + \, \left(N \, - \, \overline{N}\right) \left[\, 1 \, - \, F\left(\overline{x};\theta\right)\right] \tag{13}$$

and solution of the parameter can be found

$$\hat{\theta} \, = \, arg \min_{\theta} \left[-ln\mathcal{L}\left(\theta\right)\right] \tag{14}$$

CONCLUSIONS

In this paper, we investigate relationships between seismic action, system response and relevant damage levels in a prototype of an industrial plant. This has been possible by means of the development of a procedure that combines modeling of the industrial structure, in both primary and secondary elements, and selecting proper ground motion time histories for analyses. As a first step, we have defined a seismic scenario associated to a geographical site by means of a probabilistic seismic hazard analysis. Then, based on this analysis we provide an adequate seismic input employing a stochastic ground motion model calibrated against coherent natural seismic records. Successively, in order to select ideal signal causing desired damage in terms of limit states, a large set of synthetic time histories has been generated and assigned to a low fidelity finite element model. In particular, we focused on the modeling of secondary elements, such as elbows, tee-joints and bolted flange joints, i.e. critical elements within the steel structure. As a result, both the steel structure and relevant industrial components have been subjected to artificial spectrum-compatible and seismic records provided by a ground motion model. Thus targeted LS have been sought. Finally, we present the methodology to derive fragility curves based on the results of LF models.

ACKNOWLEDGEMENT

We wish to acknowledge the European Union's Horizon 2020 research and innovation programme under grant agreement No 730900 for funding project SPIF and EUCENTRE Fondation for access to the laboratory.

REFERENCES

[1] E. Cruz and D. Valdivia. *Performance of industrial facilities inthe chilean earthquake of 27 february 2010.* The Structural Design of Tall and Special Buildings, Vol. 20, pp. 83-101, 2011.

[2] M. Erdik and E. Uckan. *Earthquake Damage and Fragilities of Industrial Facilities*, Springer, pp. 3-13, 2014.

[3] E. Krausmann, V. Cozzani, E. Salzano, and E. Renni. *Industrial Accidents Triggered by Natural Hazards: An Emerging Risk Issue*, volume Vol.11. Natural Hazards and Earth System Sciences, 2011.

[4] M. Campedel. *Analysis of major industrial accidents triggered by natural events reported in the principal available chemical accident databases*, Technical report, JRC42281, Joint Research Centre Institute for the Protection and Security of the Citizen, Ispra, Italy, 2008. Report EUR 23391 EN - 2008.

[5] A. Cruz and N. Okada. *Consideration of Natural Hazards in the Design and Risk Management of Industrial Facilities*, Vol. 44(2):213-227 Natural Hazards, 2008.

[6] INDUSE2Safety. *Component Fragility Evaluation, Seismic Safety Assessment And Design Of Petrochemical Plants Under Design-Basis And Beyond-Design-Basis Accident Conditions*, RFS-CT-2014-00025, Work Package 4 – Deliverable D4.4.

[7] J. Baker. *Efficient Analytical Fragility Function Fitting Using Dynamic Structural Analysis*, Earthquake Spectra, 2015.

[8] T. Haukaas and A. Der Kiureghian. *Finite Element Reliabilityand Sensitivity Methods for Performance-Based Earthquake Engineering*, Technical report, PEER - Pacific Earthquake Engineering Research Center, 2004.

[9] S. Rezaeian and A. Der Kiureghian. *Stochastic Modeling and Simulation of Ground Motions for Performance-Based Earthquake Engineering*, Technical report, PEER - Pacific Earthquake Engineering Research Center, 2010.

[10] K. Porter, R. Kennedy, and R. Bachman. *Creating Fragility Function for Performance-Based Engineering*, Earthquake Spectra, 2007.

[11] S.Rezaeian and A. Der Kiureghian. *Simulation of synthetic ground motions for specified earthquake and site characteristics*, Earthquake Engineering and Structural Dynamics, (39):1155–1180, 2010.

[12] MATLAB. 9.5.0.1049112 (R2018b) Update 3. The MathWorks Inc., Natick, Massachusetts, 2018.

[13] Computer Structure, inc. *CSI Analysis Reference Manual*, November 2017.

[14] M. Vathi, S. Karamanos, I. Kapogiannis, and K. Spiliopoulos. *Performance criteria for liquid storage tanks and piping systems subjected to seismic loading*, Journal of Pressure Vessel Technology, 139, 05 2017

[15] V. La Salandra, R. di Filippo, O. Bursi, F. Paolacci, and S. Alessandri. *Cyclic response of enhanced bolted flange joints for piping systems*, PVP2016-63244.

[16] O. Kireev, D. Kireev, and A. Berkovsky. *Parametric study of flexibility factor for curved pipe and welding elbows*, 2013.

[17] H. Ebrahimian, F. Jalayer, A. Lucchini, F. Mollaioli, and G. Manfredi. *Preliminary ranking of alternative scalar and vector in-tensity measures of ground shaking*, Bulletin of Earthquake Engineering, 2015.

[18] K. Mackie and B. Stojadinovic. *Comparison of Incremental Dynamic, Cloud and Stripe Methods for Computing Probabilistic Seismic Demand Models*, ASCE: Proceedings of the 2005 Structures Congress, 2005.

[19] M. Broccardo. *Lecture notes: Principle for fragility function computation*, ETH Zürich: Probabilistic seismic risk analysis and management for civil systems, 2016.